THE JOURNAL OF PHYSICAL CHEMISTRY B

Article

pubs.acs.org/JPCB

First Principle Approach to Solvation by Methylimidazolium-Based Ionic Liquids

Elixabete Rezabal*,† and Thomas Schäfer*,†,‡

†POLYMAT, University of the Basque Country UPV/EHU, 20018 Donostia-San Sebastián, Spain

‡IKERBASQUE, Basque Foundation for Science, 48011 Bilbao, Spain

Supporting Information

ABSTRACT: Understanding the nature of the inter- and intramolecular interactions of solutes and ionic liquid (IL) ion pairs from an electronic point of view is necessary for explaining the mechanisms behind the selectivity of ILs toward a certain solute. Due to the complexity of the underlying physicochemical interactions, and aiming at a reliable representation of the solute−IL interactions, the model system chosen in this work is formed by one single ion pair and the solute of interest, in the gas phase. Ab initio molecular dynamics (MD) techniques are used for ensuring a complete scan of the potential energy surface. A representative number of structures extracted from this trajectory are optimized using more sophisticated DFT methods. Posterior bond analysis (with natural bonding orbitals (NBO), and Morokuma-like energy partition) provide a detailed picture of the solute−IL bond nature for a set of various solutes, anions, and cations, to find a relationship between the gas phase electronic characteristics and the experimentally observed behavior. The approximation to the ILs solvation properties employing this very basic model shows that, on one side, the specific interaction of the solute with methylimidazolium-based IL is a reliable indication of the overall affinity between the bulk IL and the solute, and can be considered a predictive tool for the bulk behavior. Furthermore, the systematic study carried out has permitted the rational comprehension of such properties and thus permits us to extend it to other systems.

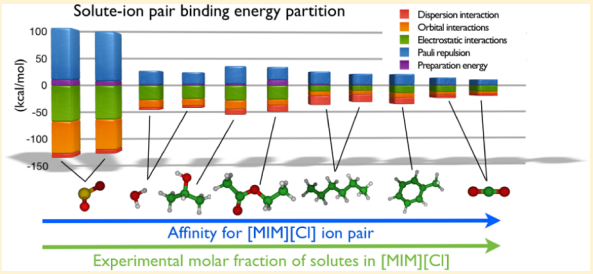

INTRODUCTION

Ionic liquids (ILs) are salts whose melting temperature is understood to be around ambient or below ambient temperature. Since the late 1990s, ILs have attracted remarkable attention from chemists due to their great potential for applications in electrochemistry, separation and extractions of chemicals and as solvent for a wide variety of chemical reactions. The diversity of these systems derives from the easy tuneability of their physicochemical properties. Typical ILs are composed of, but not limited to, an organic cation (most often an alkyl-substituted imidazolium, a pyridinium or a quaternary ammonium ion) and an inorganic anion.[1] In particular, solvent properties of methylimidazolium-based ILs have been widely studied, as media for chemical reactions and catalysis,[2] and gas separation.[3]

Apart from the wealth of experimental research conducted on the properties of methylimidazolium-based ILs,[4−22] a great effort has been made by theoreticians to provide insight into their physicochemical properties,[23,24,24−46] and, to a lesser extent, into their solvation properties.[41,47,48,50−60]

To fully benefit from this great potential, and hence, systematically design and predict the physicochemical properties of a particular IL or even select suitable ones for a specific reaction or application, it is necessary to create a link between the fundamental properties of the IL system (such as those deriving from its electronic and molecular structure) and its specific (macroscopic) physical and chemical properties.

The physical properties of the ILs stem from the particularly strong Coulomb (long-range) and dispersion (short-range) interactions between the ion pairs.[33,34] The equilibrium between these two forces results in rather flat potential energy surfaces and provides properties that fundamentally diverge from those of regular salts and solvents.[43] Besides, the capability to form a wide range of strong intermolecular interactions boosts the solubility of many compounds in ILs.[1] The direct relationship between the interaction strength—which is the result of a complex interplay of electrostatic forces, dispersion, and hydrogen bond—and solubility is nowadays still a matter of debate.[47,61]

The variety and strength of the intermolecular interactions requires big size systems to be considered as model study systems, that in turn constitute a great challenge for the quantum and theoretical chemistry methods. Quantum chemical calculations provide a rigorous representation of the interactions at an electronic level but can only deal with relatively small systems (some ion pairs at most, employing first principles molecular dynamics (FPMD)).[23,33,59] Instead, rather

Received: June 1, 2012
Revised: December 10, 2012
Published: December 15, 2012

ACS Publications © 2012 American Chemical Society

large systems can be described by classical molecular dynamics (MD), but at the cost of a less reliable, parametrized approximation and molecular level description.[34] Therefore, a bottom-up approach moving up on several scales is mandatory.

As a first step toward the comprehensive understanding of IL solvation processes, systematic ab initio computational studies of simple ion pairs will be used in this work to understand and predict selected features of ILs, and with the aim of finding a relationship between the gas phase electronic structure and the experimentally observed behavior. Ultimately, this could be used to guide the choice of an appropriate pairing before significant investment is made into synthesis and physical characterization of novel ILs.[30] Such an approximation was already reported in literature to be valid for the prediction of gas solubilities, based on specific interactions with some small solutes, namely SO_2, CO_2, and N_2;[50,51] in the present work, we try to understand the nature of the interactions between the methylimidazolium-based ILs and a set of different solutes. The systematic approach carried out permits us to single out the factors tuning the solvation preferences of the IL, such as the nature of the cation, length of the alkyl chain, characteristics of the anion, or the solute. This fundamental knowledge sets the grounds for predicting the behavior of different ILs solvated systems and sheds light into the solvation of bigger systems as DNA,[62−66] nanostructures,[2] or enzymes[67−73] in ILs, which relies on the specific interaction of the ion pairs with the individual functional groups constituting the whole system.

METHODS

Quantum chemical tools are chosen in this work to study the one-to-one interactions between the IL and the solute. The model consists of a single ion pair (1-butyl- and 1-octyl-3-methylimidazolium (Figure 1), Cl^-) and the solute (H_2O, SO_2, CO_2, 2-propanol, ethyl acetate, *n*-hexane, and toluene). The selected set of solutes includes common solvents and are representative for functional groups (alcohols, carbonyls, alkyl chains, aromatic rings) that are commonly present in bigger systems that are stable in IL solution, such as biopolymers, synthetic polymers, or nanostructures. Besides, they bear an intrinsic interest as potential pollutants of the environment as volatile organic compounds (VOCs).

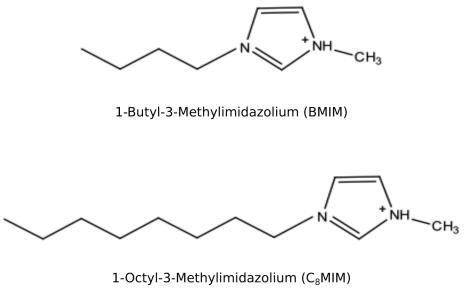

Figure 1. Cations of the ILs studied in this work.

The potential energy surface (PES) is first explored by Born−Oppenheimer molecular dynamics (MD) simulations on every [C_8MIM][Cl]−solute system (for more details, see Supporting Information). The scope of these calculations is to sample the PES and obtain a representative set of structures for posterior geometry optimization by density functional theory (DFT). In particular, among the 50 000 structures generated, each 500th is optimized, resulting in 100 structures chosen. These are then refined by DFT geometry optimizations and frequency calculations at the B3LYP-D/TZVP theory level, employing the Grimme correction[74] for the dispersion effects. The procedure resulted in at most 33 different stable minima from the initial 100 structures. The redundancy in the geometries obtained confirm the complete exploration of the potential energy surface.

Both the MD trajectories and the B3LYP-D/TZVP optimized [C_8MIM][Cl] structures showed the solute located around the anion and the ring of the cation, and therefore, no remarkable difference was expected for [BMIM][Cl]−solute systems. In fact, the configurations obtained from applying the same procedure described above to [BMIM][Cl]−H_2O and −hexane systems, were compared to those obtained by shortening the chain length of the 100 structures obtained from the MD [C_8MIM][Cl] trajectories, and optimizing them at B3LYP-D/TZVP level. No remarkable difference was obtained, as expected, in the geometries and number of stable minima found. Therefore, for the sake of computational efficiency, all the [BMIM][Cl]−solute systems were studied following the second procedure. The relative energies of the [BMIM][Cl] isomers are also available in the Supporting Information.

The affinity of the solute for the ion pair is defined as the energy balance of the reaction

$$[\mathrm{MIM}][\mathrm{Cl}] + \mathrm{solute} \rightarrow [\mathrm{MIM}][\mathrm{Cl}]-\mathrm{solute} \quad (1)$$

where the reactants are always calculated at the same theory level as the products. In the case of the [MIM][Cl] ion pair, three different configurations were found, depicted in Figure 2. In line with the literature, the global minimum presents the anion interacting with the hydrogen in C_1. Consequently, this conformer is chosen for the binding affinity calculations.

Harmonic frequency calculations are carried out, ensuring there is no imaginary modes; enthalpy and free energy values are obtained by performing a thermochemistry analysis using the standard expressions for an ideal gas in the canonical ensemble.

A Morokuma-like energy partition of the bond between the solute and the IL is posteriorly carried out, using the ADF program,[75] at the B3LYP-D/TZVP theory level, for a better understanding of the affinity and nature of the solute−ion pair interaction. This scheme allows the interaction energy to decompose between selected fragments (in this case the solute and the ion pair) into contributions associated with the various orbital and electrostatic interactions, in the framework of Kohn−Sham molecular orbital theory. The binding energy is defined as the sum of the preparation energy ΔE_{prep}, and interaction energy, ΔE_{int}:

$$\Delta E = \Delta E_{prep} + \Delta E_{int} \quad (2)$$

the preparation energy accounts for the amount of energy required to deform the separated fragments, from their equilibrium structure to the geometry they acquire in the molecule. The interaction energy is written as

$$\Delta E_{int} = \Delta E_{elst} + \Delta E_{Pauli} + \Delta E_{oi} + \Delta E_{disp} \quad (3)$$

ΔE_{elst} being the electrostatic interaction energy, which corresponds to the classical electrostatic interaction between the unperturbed charged distributions of the prepared fragments as they are brought together at their final positions. ΔE_{Pauli}, the Pauli repulsion, arises as the energy changes

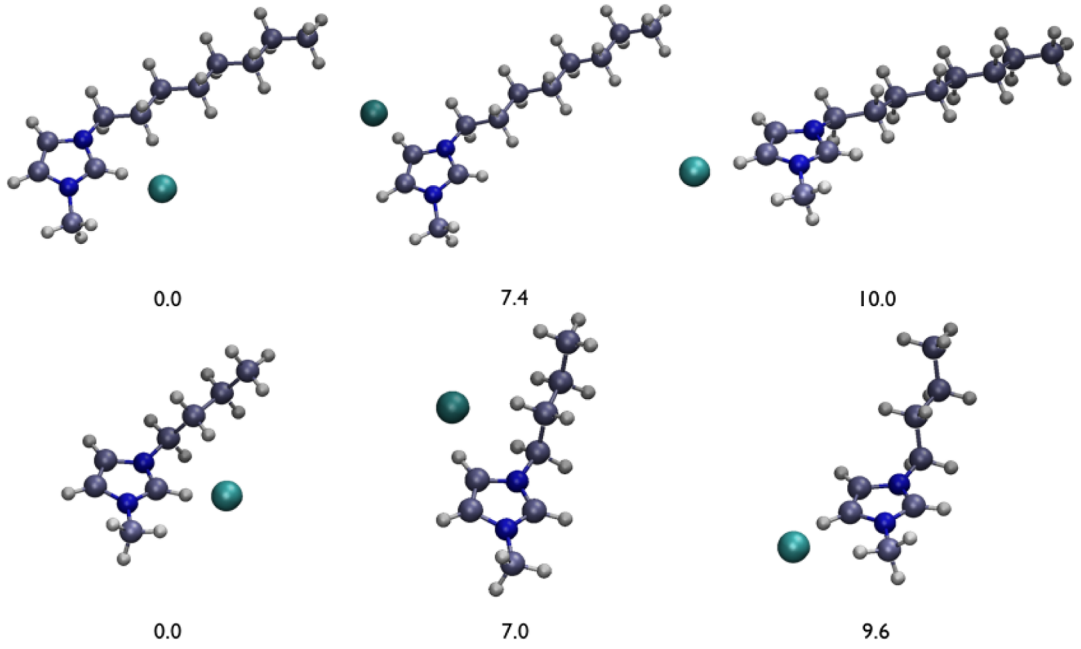

Figure 2. Different conformations of the [C_8MIM][Cl] (first row) and [BMIM][Cl] (second row) ion pairs, optimized at the B3LYP-D/TZVP level. Relative energies are given in kcal/mol.

associated with the antisymmetrization and renormalization of the wavefunction; it comprises the destabilizing interactions between occupied orbitals and is responsible for any steric repulsion. ΔE_{oi}, the orbital interaction energy, is associated to the relaxation of the wavefunction to obtain the fully converged one. It accounts for electron pair bonding, charge transfer, and polarization (defined as induction in other decomposition schemes) energies. Finally, the dispersion energy ΔE_{disp} is calculated using the empirical correction by Grimme.[74,75]

The experimental sorption of solutes by ILs is also studied, using a quartz crystal microbalance (QCM) applying a methodology reported previously in ref 76.

RESULTS

The exploration of the PES of the different solute−IL combinations by FPMD calculations and subsequent DFT optimizations pinpoint very flexible structures with a shallow potential energy surface. The anion usually locates itself around the most acidic proton of the ring (H_r), and interacts with the methyl substituents and the π cloud of the cation. The preference for this site was already observed in the literature in bare IL ion pairs.[23,25,29,30]

Efforts for locating stable minima similar to those found for the bare ion pair, where the anion interacts with the other protons of the ring, showed that these complexes lie, in fact, significantly higher in energy (around 10 kcal/mol) than those interacting with H_r, in accordance with earlier reports on [MMIM][NO_3] interaction with small solutes.[50] Therefore, in this work we will restrict ourselves to the energetically more favored low-lying minima, where the anion interacts with the H_r.

Several stable low-lying minima were identified for each solute−IL system (made available in the Supporting Information, together with the respective relative electronic energies) within a narrow energy range. H_2O, SO_2, and CO_2 establish a rather stable interaction with the anion, and consequently, show a spatial distribution around the cation very similar to that of the Cl^-. Totals of 14, 15, and 11 stable minima were identified, respectively, in an energy range of 2.3, 3.7, and 2.7 kcal/mol for [C_8MIM][Cl] and 2.2, 3.5, and 2.5 kcal/mol for [BMIM][Cl] complexes (Supporting Information, Figures S1, S2, and S3). In particular, H_2O interacts with the anion via one of the hydrogens, forming a H bond, and the anion remaining at the same plane as the solute.[41] CO_2 interacts via its C atom, resulting in a very slight deviation from linearity (6°). It remains in plane with Cl^-, as seen in the literature.[47,50] SO_2, instead, interacts with the S, the anion locating itself perpendicular to the molecular plane.

The solute (H_2O, SO_2, and CO_2)−Cl^- distance varies insignificantly for the different configurations found. They can be classified in two groups, according to the position of the anion with respect to the imidazolium ring (Figure 3): the *top* conformation presents the anion interacting with the π electron cloud of the ring with $d(H_r-Cl)$ = 2.864, 3.462, and 2.702 Å, respectively for C_8MIM structures and 2.866, 3.463, and 2.710 Å for BMIM. The *front* conformation locates the anion interacting with the proton in C_2, with $d(H_r-Cl)$ = 2.244, 2.618, and 2.105 Å for C_8MIM and 2.244, 2.608, and 2.103 Å for BMIM (Table 1).

As stated above, the different conformations do not contribute significantly to the affinity for the solute. In fact, the energy difference between the energetically most stable *top* and *front* conformations is no larger than 1.1 kcal/mol at B3LYP-D/TZVP theory level, and therefore, they should be considered thermoneutral.

Propanol, ethyl acetate, and toluene interact both with the anion and with the substituents of the cation, although the distribution is not as flexible as for the smaller solutes. Totals of 10, 16, and 5 stable minima were characterized, respectively, within an energy range of 1.7, 3.7, and 3.3 kcal/mol for [C_8MIM][Cl] and 1.5, 3.7, and 3.4 kcal/mol for [BMIM][Cl] complexes (Supporting Information, Figures S4, S5, and S6). Propanol forms a H bond with the Cl^- via the −OH group, whereas the alkyl chain can adopt various orientations without

dx.doi.org/10.1021/jp305379s | J. Phys. Chem. B 2013, 117, 553−562

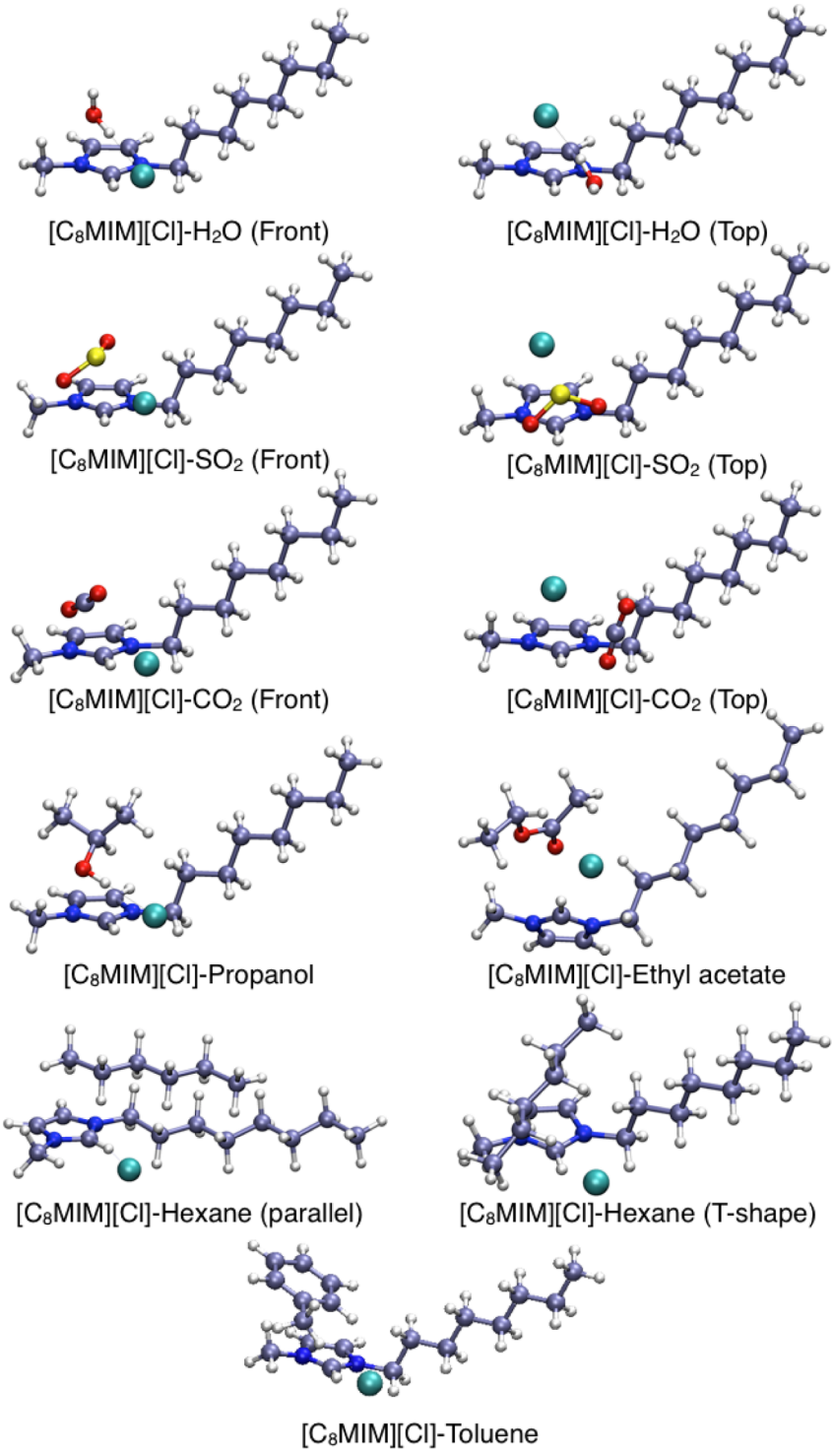

Figure 3. Most stable configurations for each solute−IL pair studied in this work, optimized at the B3LYP-D/TZVP level (see text).

any remarkable energy penalty. Ethyl acetate does not form any bond via the carbonyl oxygen but rather interacts with the anion via H bonds of the alkyl chain, the carbonyl pointing toward the cation. Similarly, toluene binds the Cl^- atom forming H bonds, mainly with the H atom in the methyl substituent, the ring oriented toward the cation (see Figure 3 for the $[C_8MIM][Cl]$ configurations).

In the case of propanol, ethyl acetate, and toluene configurations, the position of the anion with respect to the cation and the distance of the solute to the anion ($d(H_r-Cl)$ and $d(sol-Cl)$) hardly vary in the different conformations. Only the orientation of the solute with respect to the cation differs, which does not suppose a substantial affinity change. Finally, hexane is the only solute not interacting directly with the anion (as reflected in the short $d(H_r-Cl)$), but showing preference for the ring (in *T-shape*, perpendicular to the substituent chain) and the substituent chain (*parallel* to it) of the cation. A large number of low-lying stable minima (33) were characterized in this case, within a slightly larger energy gap than the other complexes, namely 4.9 in the case of

dx.doi.org/10.1021/jp305379s | J. Phys. Chem. B 2013, 117, 553−562

Table 1. Selected Geometrical Parameters (Å) (B3LYP-D/TZVP) for the Most Relevant [C_8MIM][Cl] and [BMIM][Cl] Configurations[a]

	[C_8MIM][Cl]		[BMIM][Cl]	
	$d(H_r-Cl)$	d(sol−Cl)	$d(H_r-Cl)$	d(sol−Cl)
H_2O top	2.864	2.082	2.866	2.080
H_2O front	2.244	2.108	2.244	2.107
SO_2 top	3.462	2.516	3.463	2.514
SO_2 front	2.618	2.531	2.608	2.530
CO_2 top	2.702	3.078	2.710	3.082
CO_2 front	2.105	3.092	2.103	3.095
2-propanol	2.256	2.134	2.232	2.147
ethyl acetate	2.222	2.661	2.224	2.655
n-hexane parallel	2.008	2.811	2.011	2.761
n-hexane T-shape	2.076	2.924	2.070	2.923
toluene	2.122	2.699	2.123	2.694

[a] $d(H_r-Cl)$ denotes the distance between the most acidic proton of the cation and the anion, and d(sol−Cl) stands for the shortest distance between the solute and the anion.

[C_8MIM][Cl] and 5.4 for [BMIM][Cl] complexes (Supporting Information, Figure S7).

Among the different configurations found for each complex, the energetically most stable one of each conformation is chosen for further analysis and discussion (Figure 3).

Comparing the data obtained for C_8MIM and BMIM in Table 1, it becomes clear that the length of the substituent does not substantially alter the structural characteristics of the complexes; furthermore, the chain rotates freely, except in the case of hexane.

The accurate description of weak noncovalent interactions as hydrogen bonding and dispersion interactions dominating the interactions within ILs, requires a correlated level of theory. Therefore, single point calculations on selected complexes will be carried out by employing the highly correlated CCSD(T) and MP2 post-HF methods, combined with the TZVP basis set. The performance of other approximate density functionals (DFs) with respect to the post-HF methods is assessed, to identify a reliable DF for our system. The satisfactory performance of MP2 as compared to the highly accurate, but computationally costly CCSD(T) in similar systems has been reported in the literature.[24,29,31]

Therefore, binding energies were calculated with the B3LYP-D/TZVP geometries at the CCSD(T)/TZVP and MP2/TZVP levels of theory, and the performance of M06,[77] B3LYP,[78−80] and PBE[81] (the last two with and without dispersion correction) combined with the TZVP[82,83] basis set was checked against this data (Table 2). No empirical correction was included for M06, because it already accounts for the dispersion interactions. CCSD(T)[84,85] calculations are computationally very demanding and doable only for some of the solutes, namely H_2O, SO_2, CO_2, propanol, and toluene. The reference data for ethyl acetate and hexane will be MP2, which reproduces satisfactorily the CCSD(T) results in most of the cases. As an exception, the deviation for the toluene was slightly larger but still small (−2.8 kcal/mol).

The DFs reproduced the reference data with irregular success; those accounting for the dispersion effects (M06, B3LYP-D, and PBE-D) obtained very similar results (deviations smaller than 2.5), even though they overestimate the affinity for SO_2 by 4.6−5.7 kcal/mol. Instead, B3LYP and PBE perform very satisfactorily for the small solutes (H_2O, SO_2, and CO_2), namely, those which do not bear significant dispersion interactions (deviations less than 1.9 kcal/mol) but, instead, largely underestimate the binding energy of hexane, propanol, ethyl acetate, and toluene (between 6.9 and 13.4 kcal/mol). Apart from the systematic overestimation of the SO_2 binding energy, M06, B3LYP-D, and PBE-D are the functionals providing the best and most balanced performance.

Additional geometry optimizations were carried out at each DFT level, to check the influence of the geometry chosen (B3LYP-D/TZVP) in the accuracy of the results (available in Supporting Information, Table S1). Even though the performance of B3LYP and PBE, in particular, improves the results obtained by single point calculations for those solutes presenting strongest dispersion interactions, the overall trends do not change and these functionals do not reproduce the reference values satisfactorily, as they still deviate between 6.1 and 8.5 kcal/mol from the reference value. To present a consistent comparison, and due to the high computational cost of post-HF optimizations, only the single point results are discussed throughout this work.

Therefore, considering that the deviations observed do not jeopardize the overall trend prediction with regard to solute affinity of ILs, the binding energies presented here will be obtained performing single point calculations with M06/TZVP on B3LYP-D/TZVP geometries, for the sake of computational efficiency.

The influence of the basis set superposition error (BSSE) was first checked by means of the counterpoise correction by Boys and Bernardi,[86] the most common and computationally

Table 2. Binding Energies (ΔE, kcal/mol) of the Solute to [BMIM][Cl] at the MP2 and CCSD(T) Levels, Together with the Deviations ($\Delta\Delta E$, kcal/mol) of the DFT Data from CCSD(T) or MP2 (in the Case of Ethyl Acetate and Hexane) Results, Combined with the TZVP Basis Set[a]

	ΔE		$\Delta\Delta E$				
	CCSD(T)	MP2	M06	B3LYP-D	PBE-D	B3LYP	PBE
H_2O	−16.6	−17.7	−0.1	−1.2	−1.0	1.7	1.0
SO_2	−22.2	−22.3	−4.6	−5.6	−5.7	0.3	−1.5
CO_2	−7.5	−7.9	0.4	−0.4	0.4	1.6	1.9
2-propanol	−19.1	−20.5	0.1	−0.7	−0.1	9.1	6.9
ethyl acetate		−16.2	1.1	0.7	2.2	11.9	10.2
n-hexane		−10.1	0.8	−1.3	0.1	13.4	10.6
toluene	−14.5	−17.3	2.5	0.8	1.7	11.6	9.3

[a] Negative numbers denote overestimation of the reference data. Top conformers are chosen for H_2O, SO_2, and CO_2 complexes, and the parallel conformer is chosen for hexane.

dx.doi.org/10.1021/jp305379s | J. Phys. Chem. B 2013, 117, 553−562

affordable estimation of BSSE. Even if the correction did not alter the relative affinity of the solutes toward the IL, it was found to be quite high for CCSD(T) and MP2, namely between 2.9 and 8.7 kcal/mol. On the other hand, the counterpoise correction did not exceed the 2.6 kcal/mol for any of the DFs studied, in any complex. The best way of dealing with BSSE, nevertheless, is to use a sufficiently large basis set. Because BSSE arises from the limited size of the basis set, extending its size decreases not only the BSSE but also all the errors arising from the basis set truncation. The complete basis set (CBS) limit is, therefore, BSSE free; it demands, however, a much larger computational effort than counterpoise correction and, therefore, is not well suited for a systematic study of big complexes. To check the reliability of the counterpoise correction in our systems, we performed MP2/QZVP single point calculations for the [BMIM][Cl]−ethyl acetate complex, which presented a counterpoise correction of 8.2 kcal/mol at the MP2/TZVP level. The binding energy obtained at the MP2/QZVP level is −15.0 kcal/mol, and the counterpoise correction (1.4 kcal/mol) lowers it to −13.6 kcal/mol. If the result is extrapolated to the CBS limit following the extrapolation scheme for MP2 and CCSD(T) by Helgaker and co-workers,[87] we obtain a binding energy of −14.2 kcal/mol. Compared to the MP2/TZVP binding energy (−16.2 kcal/mol) and the counterpoise corrected value at the same level (−8.0 kcal/mol), the uncorrected binding energy turns out to be more accurate (a deviation of 2 kcal/mol from the CBS value) than the counterpoise corrected value (deviation of 6.2 kcal/mol from the CBS value).

In fact, it has already been documented in the literature also for other systems (see refs 88−90 and references therein) that the counterpoise correction does not necessarily improve the uncorrected value but rather presents a higher deviation from the CBS value. Besides, the good agreement observed here between the TZVP and the CBS values does not justify the computational effort necessary for calculating CBS values at the CCSD(T) and MP2 levels for all the complexes, as the overall chemistry studied is not expected to be significantly altered. Therefore, keeping in mind that the values presented here deviate to some extent from the CBS value, the reaction energies discussed throughout the text will not be BSSE corrected.

The computed binding enthalpies and free energies (Table 3) indicate that affinity does not vary much with either the different conformation or the substituent chain length. The largest change is seen, as expected, in the hexane *parallel* conformation, which rises to a hardly significant stabilization of 1.8 kcal/mol in ΔG. Therefore, we can isolate the solute as the main factor tuning the affinity in this set of systems. Among the solutes studied here, the structure pinpoints an interaction of the solute with the anion, except for hexane, which interacts with the cation. The most favorable interaction is shown by SO_2, which bears binding enthalpies between −23.2 and −25.0 kcal/mol, followed by propanol and water, which present similar affinities for the ion pair (between −14.7 and −17.1 kcal/mol). Ethyl acetate binds weakly but still exothermically (−12.9 and −13.7 kcal/mol) and exoergically (−0.8 and −1.6 kcal/mol) to the ion pair, whereas hexane, toluene, and CO_2 show a low affinity (ΔH = −8.5, −9.5, and −6.2 kcal/mol at most, respectively), with positive binding free energies (at least 3.2, 0.5, and 1.4 kcal/mol, respectively).

To prove a systematic comparison between this prediction and its practical implications, experimental affinity measurements of the solutes for the [C_8MIM][Cl] were carried out using a QCM. Satisfactorily enough, the experimental molar fraction of solutes absorbed into the IL at saturated vapor conditions (x_{exp} in Table 3) shows the same tendencies as those predicted by theoretical calculations, validating in this way the usefulness of the theoretical approach despite of the considerably different levels of observation between the molecular model and the experimental bulk behavior of the IL.

Table 3. Binding Enthalpies (ΔH, kcal/mol) and Free Energies (ΔG, kcal/mol) of the Solute for the Most Relevant [C8MIM][Cl] and [BMIM][Cl] Configurations (M06/TZVP//B3LYP-D/TZVP) and the Experimental Molar Fractions (x_{exp}) of Each Solute in [C_8MIM][Cl], Obtained by QCM

	[C_8MIM][Cl]			[BMIM][Cl]	
	ΔH	ΔG	x_{exp}	ΔH	ΔG
H_2O top	−15.4	−5.8	0.77	−16.3	−6.5
H_2O front	−14.7	−5.0	0.77	−15.4	−6.1
SO_2 top	−24.1	−11.9		−25.0	−12.6
SO_2 front	−23.2	−11.4		−23.9	−12.1
CO_2 top	−6.2	3.5	0.03	−6.8	2.5
CO_2 front	−5.9	1.4	0.03	−6.6	0.6
2-propanol	−17.1	−5.8	0.69	−17.6	−6.0
ethyl acetate	−12.9	−0.8	0.47	−13.7	−1.6
n-hexane parallel	−8.4	5.0	0.54	−7.9	4.9
n-hexane T-shape	−8.5	3.2	0.54	−9.3	1.9
toluene	−9.5	0.5	0.19	−10.2	0.0

A further, deeper understanding on the interactions was obtained by performing the Morokuma-like bond energy partition (Table 4) and NBO analysis (Table 5). Given the small differences observed so far between the C_8MIM and BMIM data, only the energy partition of the former will be discussed in the following.

The first observation made was that the preferred solutes present substantial orbital interaction energy (ΔE_{oi}) with the ion pair (−54.9, −15.2, and −13.7 kcal/mol, respectively, for SO_2, propanol, and water); in fact, this contribution is smaller as the overall affinity of the IL for the solute decreases. Propanol and H_2O form a hydrogen bond between the −OH moiety and the anion (as observed experimentally for water and BMIM ILs[9]) whereas SO_2 establishes an interaction of the empty π^* LUMO of the solute with the doubly occupied p orbitals of Cl^-. In both cases, the interactions enable high conformational flexibility, due to the three available p orbitals of the Cl^-. The rest of the solutes do not bear remarkable orbital interaction with the ion pair, the lowest contribution being that to CO_2. NBO analysis (Table 5) is in line with these results, SO_2, H_2O, and propanol showing a greater charge transfer from the anion, reflected in the second-order orbital interactions of 32.8, 19.0−21.4, and 19.2 kcal/mol, respectively. Ethyl acetate, as expected, bears a more modest transfer (6.8 kcal/mol) but still stronger than for the rest of the solutes.

In comparison, very discrete charge transfer is observed from the solute to the cation, except in the case of SO_2, which transfers around 13 kcal/mol to the cation ring. Nevertheless, also in this case, the contribution of the anion can be considered to dominate the interaction. This is in line with the structural and energetic characteristics pointing out that the anion dominates the affinity of the solute for the ion pair.

Electrostatic interactions, as expected, are attractive in all systems. Those presenting a dipole moment bear strongest

dx.doi.org/10.1021/jp305379s | J. Phys. Chem. B 2013, 117, 553−562

Table 4. Binding Energy Partition (kcal/mol, B3LYP-D/TZVP) for [C_8MIM][Cl] Complexes, Together with the Dipole Moment (Debye) of the Solute in Each Case

	ΔE_{int}	ΔE_{prep}	ΔE_{Pauli}	ΔE_{elst}	ΔE_{oi}	ΔE_{disp}	D
H_2O top	−17.9	1.4	24.0	−24.6	−13.7	−3.6	2.147
H_2O front	−17.6	2.0	20.9	−22.6	−12.0	−3.8	2.147
SO_2 top	−35.1	9.8	88.3	−61.2	−54.9	−7.3	2.080
SO_2 front	−32.4	7.8	84.2	−57.7	−52.1	−6.9	2.080
CO_2 top	−8.9	1.0	12.9	−11.0	−4.8	−6.0	0.000
CO_2 front	−7.9	0.7	10.2	−10.2	−4.0	−3.9	0.000
2-propanol	−19.7	2.8	30.8	−25.5	−15.2	−9.8	1.713
ethyl acetate	−22.9	9.6	22.5	−23.8	−10.3	−11.3	2.043
n-hexane parallel	−11.1	1.8	22.6	−10.0	−7.9	−15.7	0.000
n-hexane T-shape	−9.4	1.3	19.1	−8.8	−6.8	−12.9	0.000
toluene	−13.2	0.8	19.3	−12.9	−8.4	−11.2	0.378

Table 5. Second-Order Orbital Interactions (kcal/mol) Obtained by NBO Analysis (M06/TZVP//B3LYP-D/TZVP) between the Solutes and the Ion Pair[a]

	E_{S-A}	E_{A-S}	E_{S-C}	E_{C-S}
H_2O top	0.1	21.4	5.6	0.3
H_2O front	0.1	19.0	2.7	0.4
SO_2 top	1.8	32.8	12.9	0.3
SO_2 front	1.5	32.8	13.0	0.3
CO_2 top		2.7	1.8	0.2
CO_2 front		2.4	1.3	
2-propanol	0.1	19.2	5.4	1.0
ethyl acetate	0.1	6.8	1.4	0.4
n-hexane parallel	0.1	3.7	2.2	2.9
n-hexane T-shape	0.1	2.0	1.5	1.4
toluene		4.7	3.1	1.3

[a] E_{S-A} denotes the second-order orbital interactions from the solute to the anion, E_{A-S} that from the anion to the solute, E_{S-C} from the solute to the cation, and E_{C-S} the one from the cation to the solute.

electrostatic interactions with the anion (Table 4) (between −61.2 and −23.8 kcal/mol), whereas hexane, toluene, and CO_2 bear much weaker charge−induced dipole interactions (−12.9 to −8.8 kcal/mol). This charge−induced dipole interaction results in the CO_2 molecule deviation from linearity by around 6°, slightly less than anion−CO_2 structures found in the literature[50] (8.52°), due to the presence of the cation. Finally, as expected, significant dispersion interactions are observed for the bulkiest ligands, namely ethyl acetate, hexane, and toluene, closely followed by propanol.

DISCUSSION

Both the FPMD and static calculations reveal a very shallow potential energy surface of the IL−solute complexes, indicating a facile motion of the solute without loss of interaction.

Alkyl chain rotation is found to vary over a large range of angles at little expense of energy and does not remarkably alter the affinity for the solutes, confirming previous observations on similar systems with CO_2 (see ref 10 and references therein).

The different solutes considered interact with the anion, with the exception of hexane, which, nevertheless, does not remarkably change its affinity when the cation is changed. This is in agreement with experimental and theoretical studies in the literature, which conclude that it is the nature of the anion that influences the solubilities of gases in methylimidazolium-based ILs, rather than the cation.[7−9,12,18,30,31,41,47,50,58,91] The origin of this preference arises from the more dispersed charge in the methylimidazolium cation, as compared to the Cl^- anion according to Klähn and co-workers.[67]

In fact, earlier theoretical data obtained considering only the solute−anion interaction, yield similar thermodynamic data as in the present manuscript, which has considered the whole ion pair. Our model predicts a H_2O−Cl^- bond distance between 2.080 and 2.108 Å (Table 1), depending on the conformation and the cation considered. The binding enthalpy, instead, is estimated to be between −14.7 and −16.3 kcal/mol, at the M06/TZVP//B3LYP-D/ TZVP level (Table 3). Wang and co-workers obtained very similar results considering only the solute−anion complex, namely a 2.184 Å bond distance distance and ΔH = −14.8 at the MP2/6-31++G* level and between −16.9 and −13.9 kcal/mol employing B3LYP combined with different basis sets.[49] Similarly, the binding energy between CO_2 and Cl^- was estimated in ΔE = −6.4 kcal/mol (Car−Parrinello MD simulations[47]) and −4.46 kcal/mol (MP2/6-311+G*[50]). These values are very close to those predicted in the present manuscript, namely ΔE = −6.4 kcal/mol (CCSD(T)/TZVP, Table 2).

In summary, it can be assumed that in these systems, the affinity of the solutes is mainly dictated by the physical nature of the different interactions that take place between an ion and a neutral molecule, i.e., specific orbital interactions, charge−dipole, charge−induced dipole, and dispersion interactions, in decreasing order of influence.

Among the solutes considered here, SO_2 shows the strongest orbital interaction, and therefore the highest solubility is expected (binding enthalpy around 24 kcal/mol). In fact, the extremely high solubility of SO_2 in comparison to CO_2 was already reported experimentally and theoretically in bulk IL.[14,20,50,55] Propanol and H_2O form H bonds with the anion (as confirmed experimentally[9]) and bear very similar affinities (of about ΔH = −17 kcal/mol and ΔH = −15 kcal/mol, respectively), enhanced in the former due to the dispersion interaction. We should expect similar affinities for any alcohol or −OH group integrated in a bigger structure. Accordingly, CBS-QB3 data[59] predicts ΔH = −14.36 kcal/mol and ΔG = −5.21 kcal/mol for [C_8MIM][Cl]−methanol, in very good agreement with our data.

Those solutes that do not bind the anion via a H bond are only ligated via charge−dipole interaction. The strength of this interaction will decrease with the respective dipole moment (Table 4), namely ethyl acetate > toluene > CO_2 = hexane. Toluene, CO_2, and hexane, with weak or zero dipoles, are not likely to bind strongly the ion pair (around ΔH = 9 kcal/mol,

dx.doi.org/10.1021/jp305379s | J. Phys. Chem. B 2013, 117, 553−562

Table 6. Binding Enthalpies (ΔH, kcal/mol) and Free Energies (ΔG, kcal/mol) for CO_2 and [C_8MIM][X], X Being the Different Anions Considered (M06/TZVP//B3LYP-D/TZVP), and the Deviation from Linearity in the CO_2 Molecule (α, deg)

X	ΔH	ΔG	ΔE_{int}	ΔE_{prep}	ΔE_{Pauli}	ΔE_{elst}	ΔE_{oi}	ΔE_{disp}	α
Cl^-	−6.2	3.5	−8.9	1.0	12.9	−11.0	−4.8	−6.0	6
BF_4^-	−4.7	5.3	−7.1	0.2	7.7	−7.4	−2.8	−4.6	3
PF_6^-	−4.4	4.6	−6.5	0.8	6.6	−6.2	−2.9	−4.0	2

ΔH = 6 kcal/mol, and ΔH = 8 kcal/mol and exoergic binding free energies), because they rely only on charge−induced dipole and dispersion interactions. Similarly, low dipole moment aromatic rings and alkyl chains will contribute weakly to the interactions with methylimidazolium-based ILs. This is in agreement with the CBSQB3 calculations, which find ΔH = −6.93 kcal/mol and ΔG = 1.73 kcal/mol, for toluene,[59] or ΔH = −8.2 kcal/mol and ΔG = −0.4 kcal/mol, for benzene using Car−Parrinello MD.[8]

These findings also explain why the solubility has been found to be proportional to the polarizability of the solute, except in the case of water and CO_2,[8] or why experimental works report CO_2 affinity not to be proportional to hydrogen bond basicity of the anion.[12] Water, besides and more importantly than charge−dipole interactions, binds via H bond to the anion; CO_2, however, lacks both these interactions. As a consequence, charge−induced dipole interactions modulate its solubility in methylimidazolium-based ILs, as also suggested by the observation that the extent of the distortion of CO_2 from a linear geometry upon complexation is roughly proportional to the binding energy.[47]

In such cases, other factors may influence the adsorption of CO_2 as much as the binding energy, as suggested in the literature, and extending the system to several IL ion pairs might be crucial to understand their precise role. Nevertheless, these factors do not seem likely to greatly improve the adsorption at room temperature, as compared to other solutes,[10] considering our theoretical and experimental data. The latter is particularly interesting as it does not confirm the common opinion that methylimidazolium-based ILs have in general a high affinity for CO_2.

The same line of reasoning can be followed for predicting the affinity for other anions such as BF_4^- and PF_6^-, which are widely used and investigated. The potential generated by a charge distribution is proportional to the charge distribution and inversely proportional to the radius. In the present case, both BF_4^- and PF_6^- have the same charge and much larger radius than Cl^- and, therefore, are expected to exert weaker charge−dipole and charge−induced dipole interactions.

The affinities of the different ion pair combinations for CO_2, together with the bond energy partition are summarized in Table 6. This solute was chosen due to the extensive research conducted on MIM BF_4^-/ PF_6^-−CO_2 systems. As expected, the affinity decreases from Cl^- to BF_4^- and PF_6^-, due to the decrease of the electrostatic interactions. The smaller charge−induced dipole interaction can also be checked by considering the deviation from linearity in the CO_2 molecule, which follows the expected trend[50] and was experimentally documented by ATR-RI spectroscopy.[7]

The summation of all these effects results in less affinity of CO_2 for BF_4^- and PF_6^- as compared to Cl^-. Other theoretical and experimental data concur with such an observation, considering only one ion pair (ΔE = −6.4, −4.8, and −3.4 kcal/mol for Cl^-, BF_4^-, and PF_6^-, respectively[47]), the bulk IL employing MD simulations (ΔH = −3.8 and ΔG = −0.1 kcal/mol for both, BF_4^- and PF_6^-, at ambient temperature[91]) or experimental measurements (−3.3 and −3.4 for BF_4^- and PF_6^-, respectively[8]). The agreement in enthalpies and free energies is very satisfactory, considering the different approaches taken and being aware of the fact that in our calculations an overestimation of the entropy must be accounted for.

A similar trend can be predicted for the other solutes included in this study, as long as they do not establish additional specific orbital interactions with the anion. In fact, the same tendency was observed experimentally[8,11] and theoretically[41] for water and alcohols;[13,59] experimentally, SO_2 molar fractions of 0.713 and 0.532 were observed at 45 C for BF_4^- and PF_6^-, respectively.[19] Following this trend, we could expect a much higher molar fraction in Cl^-, which fits well in our experimental measurements.

Among the solutes studied in this work, significant differences in the binding energies suggest that a selective extraction of SO_2 and, to a lesser extent, water and alcohols such as propanol might be possible, and that the absorption of CO_2 and hexane by the studied ILs would be, if any, a consequence of cooperative effects of several ion pairs. Besides, substituting Cl^- with BF_4^- or PF_6^- would not improve the selectivity toward CO_2 as compared to other solutes.

The significant affinity shown by water suggests that its presence in the methylimidazolium-based IL cannot be ruled out in any case, in line with the hygroscopic nature of ILs revealed in the literature;[9−11] in fact, its presence could influence the solubility of other solutes[7,10] and has also been reported to have a role in the enzymatic activity.[62,68] This seemingly obvious conclusion must strongly be taken into account as it ultimately implies that removal of residual water from ILs for sensing or separation applications can be a challenging task and might even not be feasible.

Beyond the solutes chosen here, this study also contributes to the understanding of solvation of bigger systems by methylimidazolium-based ILs. The preference of the solute for the anion explains the crucial role the anion plays in the methylimidazolium-based ILs during enzyme and DNA solvation, where the nature of the anion interaction is seen to denature or stabilize proteins, by forming H bonds[62,67] and depending on the degree of interaction.

Furthermore, the same patterns can be found in other systems such as single wall carbon nanotubes (SWCN) dispersed in methylimidazolium-based ILs, with BF_4^- and PF_6^-, and where the differences in experimental observations were related exclusively to the anions, which is in perfect agreement with our conclusions.

In fact, our calculations suggest that −OH or $-NH_2$ groups integrated in alkyl chains or aromatic rings will interact with the anions, via H bonds if possible, or only charge−dipole interactions otherwise. Unsubstituted or carbonyl substituted alkyl chains or aromatic rings are not likely to establish significant interactions with the methylimidazolium-based IL. Accordingly, and regarding the particular case of DNA solvation by methylimidazolium-based ILs, Cardoso and co-

dx.doi.org/10.1021/jp305379s | J. Phys. Chem. B 2013, 117, 553−562

workers,[64] among others,[63] have reported that the anion interacts with the DNA base pairs, whereas the cation interacts mainly with the negatively charged phosphate, dominated by Coulomb interactions. Nevertheless, in the same work, the interaction of the alkyl side chain of the cation is suggested to undergo electrostatic interactions with the aromatic base pairs of the DNA chain; this hypothesis finds no support in our work, and we suggest that this interactions would be less favorable than charge−dipole interactions between, for example, the methylimidazolium ring or the anions not interacting with the phosphates, and the $-NH_2$ groups in the bases.

CONCLUDING REMARKS

The approximation to the ILs solvation properties employing a very basic model has shown that, on one side, the specific interaction of the solute with methylimidazolium-based IL is a reliable indication of the overall affinity between the IL and the solute and can therefore be considered a predictive tool for the experimental behavior. Furthermore, the systematic study carried out has permitted the rational comprehension of such properties and thus allows extending them to other systems. The preliminary calculations done with different density functionals point out, however, that DFs which do not consider dispersion effects should be carefully handled, because significant deviations may arise from this omission.

In summary, in this work we have outlined the factors that dominate the solvation by methylimidazolium ILs. Even though a limited model system is employed, we have shown that basic principles constitute a predictive tool that can also be extended and integrated in more complex systems.

ASSOCIATED CONTENT

Supporting Information

Relative stabilities and geometries of all optimized configurations for each complex studied, binding energies, and MD calculation information. This material is available free of charge via the Internet at http://pubs.acs.org.

AUTHOR INFORMATION

Corresponding Author

*E-mail: E.R., elixabete.rezabal@ehu.es; T.S., thomas_schafer@ehu.es.

Notes

The authors declare no competing financial interest.

ACKNOWLEDGMENTS

This research was funded by the ERC Starting Grant 209842-MATRIX (T.S.). Technical and human support provided by IZO-SGI, SGIker (UPV/EHU, MICINN, GV/EJ, ERDF, and ESF), is gratefully acknowledged for assistance and generous allocation of computational resources.

REFERENCES

(1) Moniruzzaman, M.; Nakashima, K.; Kamiya, N.; Goto, M. *Biochem. Eng. J.* **2010**, *48*, 295−314.
(2) Wang, J.; Chu, H.; Li, Y. *ACS Nano* **2008**, *2*, 2540−2546.
(3) Mutelet, F.; Jaubert, J. N. In *Ionic Liquids: Theory, Properties, New Approaches*; Kokorin, A., Ed.; InTech: Rijeka, Croatia, 2008; pp 225−244.
(4) Aparicio, S.; Atilhan, M. *Energy Fuels* **2010**, *24*, 4989−5001.
(5) Endo, T.; Kato, T.; Nishikawa, K. *J. Phys. Chem. B* **2010**, *114*, 9201−9208.
(6) Zvereva, E. E.; Katsyuba, S. A.; Dyson, P. J. *Phys. Chem. Chem. Phys.* **2010**, *12*, 13780−13787.
(7) Kazarian, S. G.; Briscoe, B. J.; Welton, T. *Chem. Commun.* **2000**, 2047−2048.
(8) Anthony, J. L.; Anderson, J. L.; Maginn, E. J.; Brennecke, J. F. *J. Phys. Chem. B* **2005**, *109*, 6366−6374.
(9) Cammarata, L.; Kazarian, S. G.; Salter, P. A.; Welton, T. *Phys. Chem. Chem. Phys.* **2001**, *3*, 5192−5200.
(10) Blanchard, L. A.; Gu, Z.; Brennecke, J. F. *J. Phys. Chem. B* **2001**, *105*, 2437−2444.
(11) Seddon, K. R.; Stark, A.; Torres, M. J. *Pure Appl. Chem.* **2000**, *72*, 2275−2287.
(12) Aki, S. N. V. K.; Mellein, B. R.; Saurer, E. M.; Brennecke, J. F. *J. Phys. Chem. B* **2004**, *108*, 20355−20365.
(13) Huang, J.; Riisager, A.; Wasserscheid, P.; Fehrmann, R. *Chem. Commun.* **2006**, *38*, 4027−4029.
(14) Anderson, J. L.; Dixon, J. K.; Maginn, E. J.; Brennecke, J. F. *J. Phys. Chem. B* **2006**, *110*, 15059−15062.
(15) Seki, T.; Grunwaldt, J. D.; Baiker, A. *J. Phys. Chem. B* **2009**, *113*, 114−122.
(16) Berg, R. W.; Deetlefs, M.; Seddon, K. R.; Shim, I.; Thompson, J. M. *J. Phys. Chem. B* **2005**, *109*, 19018−19025.
(17) Rodrigues, F.; Galante, D.; Do Nascimento, G. M.; Santos, P. S. *J. Phys. Chem. B* **2012**, *116*, 1491−1498.
(18) Anderson, J. L.; Ding, J.; Welton, T.; Armstrong, D. W. *J. Am. Chem. Soc.* **2002**, *124*, 14247−14254.
(19) Ren, S.; Hou, Y.; Wu, W.; Liu, Q.; Xiao, Y.; Chen, X. *J. Phys. Chem. B* **2010**, *114*, 2175−2179.
(20) Yokozeki, A.; Shiflett, M. B. *Energy Fuels* **2009**, *23*, 4701−4708.
(21) Wu, W.; Han, B.; Gao, H.; Liu, Z.; Jiang, T.; Huang, J. *Angew. Chem., Int. Ed.* **2004**, *43*, 2415−2417.
(22) D'Angelo, P.; Zitolo, A.; Migliorati, V.; Bodo, E.; Aquilanti, G.; Hazemann, J. L.; Testemale, D.; Mancini, G.; Caminiti, R. *J. Chem. Phys.* **2011**, *135*, 074505−074511.
(23) Kossmann, S.; Thar, J.; Kirchner, B.; Hunt, P. A.; Welton, T. *J. Chem. Phys.* **2006**, *124*, 174506−174517.
(24) Izgorodina, E. I.; Bernard, U. L.; MacFarlane, D. R. *J. Phys. Chem. A* **2009**, *113*, 7064−7072.
(25) Schmidt, J.; Krekeler, C.; Dommert, F.; Zhao, Y.; Berger, R.; Delle Site, L.; Holm, C. *J. Phys. Chem. B* **2010**, *114*, 6150−6155.
(26) Verevkin, S. P.; Emel'yanenko, V. N.; Zaitsau, D. H.; Heintz, A.; Muzny, C. D.; Frenkel, M. *Phys. Chem. Chem. Phys.* **2010**, *12*, 14994−5000.
(27) Song, Z.; Wang, H.; Xing, L. *J. Solution Chem.* **2009**, *38*, 1139−1154.
(28) Gutowski, K. E.; Holbrey, J. D.; Rogers, R. D.; Dixon, D. A. *J. Phys. Chem. B* **2005**, *109*, 23196−23208.
(29) Tsuzuki, S.; Tokuda, H.; Mikami, M. *Phys. Chem. Chem. Phys.* **2007**, *9*, 4780−4784.
(30) Hunt, P. A.; Kirchner, B.; Welton, T. *Chem.—Eur. J.* **2006**, *12*, 6762−6775.
(31) Tsuzuki, S.; Tokuda, H.; Hayamizu, K.; Watanabe, M. *J. Phys. Chem. B* **2005**, *109*, 16474−16481.
(32) Li, X.; Liu, L.; Schlegel, H. B. *J. Am. Chem. Soc.* **2002**, *124*, 9639−9647.
(33) Izgorodina, E. I. *Phys. Chem. Chem. Phys.* **2011**, *13*, 4189−4207.
(34) Wendler, K.; Dommert, F.; Zhao, Y. Y.; Berger, R.; Holm, C.; Delle Site, L. *Faraday Discuss.* **2012**, *154*, 111−132.
(35) Bühl, M.; Chaumont, A.; Schurhammer, R.; Wipff, G. *J. Phys. Chem. B* **2005**, *109*, 18591−18599.
(36) Bhargava, B.; Balasubramanian, S. *Chem. Phys. Lett.* **2006**, *417*, 486−491.
(37) Ballone, P.; Cortes-Huerto, R. *Faraday Discuss.* **2012**, *154*, 373−389.
(38) Salanne, M.; Siqueira, L. J. A.; Seitsonen, A. P.; Madden, P. A.; Kirchner, B. *Faraday Discuss.* **2012**, *154*, 171−188.
(39) Del Pópolo, M. G.; Lynden-Bell, R. M.; Kohanoff, J. *J. Phys. Chem. B* **2005**, *109*, 5895−5902.
(40) Ludwig, R. *Phys. Chem. Chem. Phys.* **2008**, *10*, 4333−4339.

(41) Wang, Y.; Li, H.; Han, S. *J. Chem. Phys.* **2006**, *124*, 44504−44511.
(42) Lehmann, S. B. C.; Roatsch, M.; Schoppke, M.; Kirchner, B. *Phys. Chem. Chem. Phys.* **2010**, *12*, 7473−7486.
(43) Zahn, S.; Uhlig, F.; Thar, J.; Spickermann, C.; Kirchner, B. *Ang. Chem. Int. Ed.* **2008**, *47*, 3639−3641.
(44) Maginn, E. J. *Acc. Chem. Res.* **2007**, *40*, 1200−1207.
(45) Hantal, G.; Cordeiro, M. N. D. S.; Jorge, M. *Phys. Chem. Chem. Phys.* **2011**, *13*, 21230−21232.
(46) Bodo, E.; Gontrani, L.; Caminiti, R.; Plechkova, N. V.; Seddon, K. R.; Triolo, A. *J. Phys. Chem. B* **2010**, *114*, 16398−16407.
(47) Bhargava, B.; Balasubramanian, S. *Chem. Phys. Lett.* **2007**, *444*, 242−246.
(48) Jamroz, M. H.; Dobrowolski, J. Cz.; Bajdor, K.; Borowlak, M. A. *J. Mol. Struct.* **1995**, *349*, 9−12.
(49) Wang, Y.; Li, H.; Han, S. *J. Phys. Chem. B* **2006**, *110*, 24646−24651.
(50) Prasad, B. R.; Senapati, S. *J. Phys. Chem. B* **2009**, *113*, 4739−4743.
(51) Teague, C. M.; Dai, S.; Jiang, D. E. *J. Phys. Chem. A* **2010**, *114*, 11761−11767.
(52) Zhu, X.; Lu, Y.; Peng, C.; Hu, J.; Liu, H.; Hu, Y. *J. Phys. Chem. B* **2011**, *115*, 3949−3958.
(53) Umebayashi, Y.; Hamano, H.; Tsuzuki, S.; Canongia Lopes, J. N.; Pádua, A. A. H.; Kameda, Y.; Kohara, S.; Yamaguchi, T.; Fujii, K.; Ishiguro, S. I. *J. Phys. Chem. B* **2010**, *114*, 11715−11724.
(54) Bhargava, B. L.; Balasubramanian, S. *J. Phys. Chem. B* **2007**, *111*, 4477−4487.
(55) Ando, R. A.; Siqueira, L. J. A.; Bazito, F. C.; Torresi, R. M.; Santos, P. S. *J. Phys. Chem. B* **2007**, *111*, 8717−8719.
(56) Shi, W.; Maginn, E. J. *J. Phys. Chem. B* **2008**, *112*, 2045−2055.
(57) Manan, N. A.; Hardacre, C.; Jacquemin, J.; Rooney, D. W.; Youngs, T. G. A. *J. Chem. Eng. Data* **2009**, *54*, 2005−2022.
(58) Huang, X.; Margulis, C. J.; Li, Y.; Berne, B. J. *J. Am. Chem. Soc.* **2005**, *127*, 17842−17851.
(59) Gao, T.; Andino, J. M.; Alvarez-Idaboy, J. R. *Phys. Chem. Chem. Phys.* **2010**, *12*, 9830−9838.
(60) Wick, C. D.; Chang, T. M.; Dang, L. X. *J. Phys. Chem. B* **2010**, *114*, 14965−14971.
(61) Hu, Y. F.; Liu, Z. C.; Xu, C. M.; Zhang, X. M. *Chem. Soc. Rev.* **2011**, *40*, 3802−3823.
(62) Micaêlo, N. M.; Soares, C. M. *J. Phys. Chem. B* **2008**, *112*, 2566−2572.
(63) Ding, Y.; Zhang, L.; Xie, J.; Guo, R. *J. Phys. Chem. B* **2010**, *114*, 2033−2043.
(64) Cardoso, L.; Micaelo, N. M. *ChemPhysChem* **2011**, *12*, 275−277.
(65) Tateishi-Karimata, H.; Sugimoto, N. *Ang. Chem. Int. Ed.* **2012**, *10*, 1416−1419.
(66) Xie, Y. N.; Wang, S. F.; Zhang, Z. L.; Pang, D. W. *J. Phys. Chem.B* **2008**, *112*, 9864−9868.
(67) Klähn, M.; Lim, G. S.; Seduraman, A.; Wu, P. *Phys. Chem. Chem. Phys.* **2011**, *13*, 1649−1662.
(68) Laszlo, J. A.; Compton, D. L. *Biotechnol. Bioeng.* **2001**, *75*, 181−186.
(69) Page, T. A.; Kraut, N. D.; Page, P. M.; Baker, G. A.; Bright, F. V. *J. Phys. Chem. B* **2009**, *113*, 12825−12830.
(70) Byrne, N.; Wang, L. M.; Belieres, J. P.; Angell, C. A. *Chem. Commun.* **2007**, 2714−2716.
(71) Byrne, N.; Angell, C. A. *J. Mol. Biol.* **2008**, *378*, 707−714.
(72) Fujita, K.; MacFarlane, D. R.; Forsyth, M. *Chem. Commun.* **2005**, 4804−4806.
(73) Vijayaraghavan, R.; Izgorodin, A.; Ganesh, V.; Surianarayanan, M.; Macfarlane, D. R. *Ang. Chem. Int. Ed.* **2010**, *49*, 1631−1633.
(74) Grimme, S. *J. Comput. Chem.* **2006**, *27*, 1787−1799.
(75) Velde, G. T. E.; Bickelhaupt, F. M.; Baerends, E. J.; Fonseca-Guerra, C.; van Gisbergen, S. J. A.; Snijders, J. G.; Ziegler, T. *J. Comput. Chem.* **2001**, *22*, 931−967.
(76) Schäfer, T.; Di Francesco, F.; Fuoco, R. *Microchem. J.* **2007**, *85*, 52−56.
(77) Zhao, Y.; Truhlar, D. G. *Theor. Chem. Acc.* **2008**, *120*, 215−241.
(78) Becke, A. D. *Phys. Rev.* **1988**, *38*, 3098−3100.
(79) Lee, C.; Yang, W.; Parr, R. G. *Phys. Rev. B* **1988**, *37*, 785−789.
(80) Stephens, P. J.; Devlin, F. J.; Chabalowski, C. F.; Frisch, M. J. *J. Phys. Chem.* **1994**, *98*, 11623−11627.
(81) Perdew, J. P.; Burke, K.; Ernzerhof, M. *Phys. Rev. Lett.* **1996**, *77*, 3865−3868.
(82) Schafer, A.; Huber, C.; Ahlrichs, R. *J. Chem. Phys.* **1994**, *100*, 5829−5835.
(83) Schafer, A.; Horn, H.; Ahlrichs, R. *J. Chem. Phys.* **1992**, *97*, 2571−2577.
(84) Raghavachari, K.; Trucks, G. W.; Pople, J. A.; Head-Gordon, M. *Chem. Phys. Lett.* **1989**, *157*, 479−483.
(85) Watts, J. D.; Gauss, J.; Bartlett, R. J. *J. Chem. Phys.* **1993**, *98*, 8718−8733.
(86) Boys, S. F.; Bernardi, F. *Mol. Phys.* **1970**, *19*, 553−566.
(87) Helgaker, T.; Klopper, W.; Koch, H. *J. Chem. Phys.* **1997**, *106*, 9639−9646.
(88) Alvarez-Idaboy, J. R.; Galano, A. *Theor. Chem. Acc.* **2010**, *126*, 75−85.
(89) Liedl, K. R. *J. Chem. Phys.* **1998**, *108*, 3199−3204.
(90) Walczak, K.; Friedrich, J.; Dolg, M. *J. Chem. Phys.* **2011**, *135*, 134118−134129.
(91) Cadena, C.; Anthony, J. L.; Shah, J. K.; Morrow, T. I.; Brennecke, J. F.; Maginn, E. J. *J. Am. Chem. Soc.* **2004**, *126*, 5300−5308.